

Solubility of Water in CO₂ Mixtures at Pipeline Operation Conditions

Mohammad Ahmad, Sander Gersen, Erwin Wilbers

Abstract—Carbon capture, transport and underground storage have become a major solution to reduce CO₂ emissions from power plants and other large CO₂ sources. A big part of this captured CO₂ stream is transported at high pressure dense phase conditions and stored in offshore underground depleted oil and gas fields. CO₂ is also transported in offshore pipelines to be used for enhanced oil and gas recovery. The captured CO₂ stream with impurities may contain water that causes severe corrosion problems, flow assurance failure and might damage valves and instrumentations. Thus, free water formation should be strictly prevented. The purpose of this work is to study the solubility of water in pure CO₂ and in CO₂ mixtures under real pipeline pressure (90-150 bar) and temperature operation conditions (5-35°C). A set up was constructed to generate experimental data. The results show the solubility of water in CO₂ mixtures increasing with the increase of the temperature or/and with the increase in pressure. A drop in water solubility in CO₂ is observed in the presence of impurities. The data generated were then used to assess the capabilities of two mixture models: the GERG-2008 model and the EOS-CG model. By generating the solubility data, this study contributes to determine the maximum allowable water content in CO₂ pipelines.

Keywords—Carbon capture and storage, water solubility, equation of states.

I. INTRODUCTION

DIFFERENT techniques, such as "post-combustion", "pre-combustion" and "oxy-fuel" are used to capture CO₂ from large point sources such as coal and gas fired power plants, and refineries. The capture results in certain impurities like nitrogen, argon, oxygen, water and some toxic elements like sulfur and nitrogen oxides, the types and quantities of which depend on the type of fuel and the capture process [1]. The presence of impurities in the CO₂ stream will deform the liquid-vapor phase boundary and may cause expansion of the two phase regime which is unwanted by CO₂ pipeline operators who seek to avoid any change in phase in their pipelines [2], [3].

The presence of free water, on the other hand, is even more critical for pipeline transport, mainly because of risks of corrosion in the pipeline. Requirements for CO₂ purity will impact the degree of purification and the costs for CO₂

separation. In the presence of free water, CO₂ dissolves in the aqueous phase and will partly ionize to form a weak acid. CO₂ slowly dissolves in water and forms carbonic acid when partly hydrated. Experience from existing pipelines shows that the corrosion rates are very low if the CO₂ is sufficiently dry. Corrosion rates can be in the order of mm per year when free water is present [4]. A typical allowable specification for water in a CO₂ pipeline with a good safety margin for avoiding corrosion is 500ppm [5]. Mohitpour et al. [6] also recommend that the allowed water content should be no more than 300 to 500ppm for CO₂ transmission in carbon steel pipelines. However, other experts argue that full dehydration should be obtained, which is generally achieved through 50ppm water content, or a concentration no more than 60% of the dew point in the worst conditions [7]. The solubility of water in CO₂ should therefore be well known. The solubility limit could change when other impurities are present [8] and [9]. There are very few experimental data available in the literature on the solubility of water in CO₂. Generating data especially at pipeline operation conditions is of a high importance for the designers and the operators of the CO₂ pipeline transmission systems and for the modeling community.

In this study, the solubility of water in pure CO₂ as well as in CO₂ mixtures is studied. The complexity of the experimental investigation resides in several issues: First, the use of a dew-point sensor with high reliability, consistency and traceability. Different types of sensors and technologies were investigated before selecting a silicon chip based sensor which shows very rapid response and better accuracy to humidity changes and is quite insensitive to sample flow rate. Second, the presence of a test rig which provides flexibility in supplying CO₂ mixtures of certain known prepared composition and controlled pressure and temperature value. A dedicated set up was constructed with more description given in the following section. Third, the water has high polar and wall stickiness properties which could cause corrosion and also disturb the homogeneity of the flow. A well attention had to be made to the set up material with the sealing, fittings, tubing and the sampling process. The experimental data generated were compared to two modern mixture models explicit in the Helmholtz free energy. The first is the GERG-2008 model [10] that was developed for the description of natural gas mixtures and is capable to describe the CO₂ mixtures studied in this work as well. The second is the EOS-CG model [11] that is based on the same mathematical structure as the GERG-2008, but was developed with special focus on CO₂ mixtures and humid gases.

Mohammad Ahmad is with DNV-GL Oil & Gas, 17 Energieweg 9743 AN Groningen (phone: 0031.50.7009767; fax: 0031.50.7009858; e-mail: mohammad.ahmad@dnvgl.com).

Sander Gersen is with DNV-GL Oil & Gas, 17 Energieweg 9743 AN Groningen (phone: 0031.50.7009775; fax: 0031.50.7009858; e-mail: sander.gersen@dnvgl.com).

Erwin Wilbers is with the Chemical Engineering Department, University of Groningen, 9712 CP Groningen, The Netherlands (e-mail: e.wilbers@rug.nl).

II. EXPERIMENTAL TEST SET UP

The experimental investigation was carried out using a high pressure reactor in which CO₂ mixtures were prepared, and where pressure and temperature were controlled and varied. The reactor is made up of a cylindrical sapphire tube (Fig. 1) that is closed by two lids and covered by a double jacket made up of polycarbonate. The temperature inside the reactor was controlled using water filled refrigerated and heating circulator connected to the double jacket around the reactor, allowing a temperature variation from 4 to 40°C. A piston system was installed inside the sapphire to provide the volume variation capability and consequently an option to vary the pressure inside the reactor. The piston was actuated by a manual capstan giving the precise position of the piston. The total volume of the reactor is 15ml. The capstan was placed vertically so that a stirrer (magnetic rod) was installed at the bottom lid of the cell for mixing purposes.

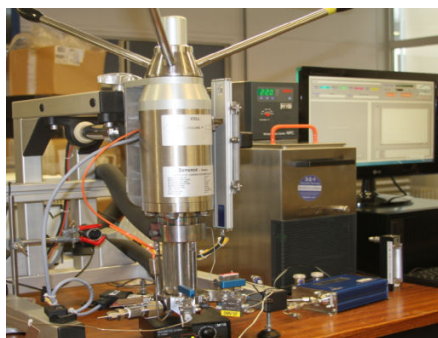


Fig. 1 Photo of the experimental system

The CO₂ is supplied to the reactor using a pump (head pressure of 200 bar). Impurities are supplied to the reactor using high pressure bottles. Water is injected using small syringes at low pressure (1 bar) inside a heated line and then is flushed into the reactor. The internal walls of the reactor are well treated to eliminate any water stickiness problems. Fig. 2 shows a schematic representation of the high pressure reactor. Pressure was measured with precise pressure transmitters in two locations, at the syringe pump side and inside the reactor side at the gage block location. The gage block contains a safety valve that opens when over pressurization inside the system occurs. The capillary connection lines had very small volumes compared to that of the reactor and the syringe pump. A set of standard high pressure (rated 1000 bar) valves was installed allowing a certain connection and isolation flexibility of the reactor, the syringe pump and the supply source.

The water content in the samples taken from the reactor through a heated line is measured using a silicon chip hygrometer. The accuracy of the hygrometer is 0.5%. 50ml/min of vapor supply is needed to get the water content value. The characteristics of the sensor are that it acts as a capacitor which interacts at the dielectric level with the hydrogen bonding of water to cause a dielectric change. The sensor is self-heating and controlled at 45°C +/-0.1°C allowing drying from the absorbed moisture every time a sample from the reactor is taken. The sensor responds to water

vapor pressure in equilibrium, thus flushing using dry nitrogen is done every time the sensor is used. The vapor exit vent is to atmosphere with no back pressure needed.

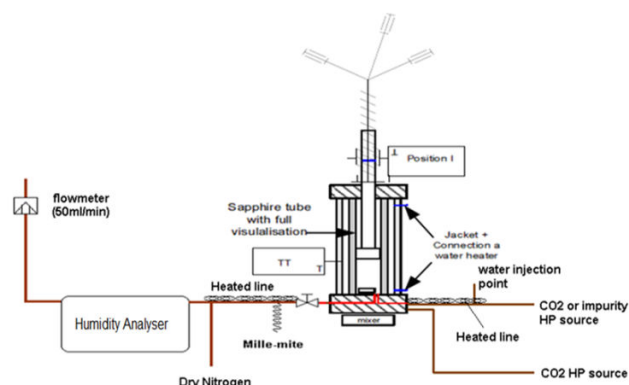


Fig. 2 Schematic representation of the experimental system

III. MEASUREMENT PROCEDURE

Before starting with the preparation of the mixtures with known compositions, the reactor was first filled with pure CO₂, heated and flushed for a couple of times to insure the elimination of any water residuals in the system. The mixtures of water and/or impurities in pure CO₂ could be then prepared inside the reactor. The water is first injected (using a hand syringe) inside the heated reactor supply line (kept at 80°C) and driven into the reactor using either the pure CO₂ supply stream (experiments with pure CO₂-water mixtures) from the pump or the impurity stream (experiments with CO₂-impurity-water) from the high pressure bottles.

Knowing the reactor volume, the initial pressure and temperature of the mixture and the mixture composition (pure CO₂ or CO₂-impurity mixture) enables us to deduce the amount of water to be injected and the injection pressure value of the impurity. The mixture prepared in the reactor is then left to homogenize using the stirrer for a couple of hours at high temperature (40°C) that provides high water solubility conditions. At the end of sample preparation phase, the mixtures prepared inside the reactor will have a known water mass content (soluble), a known mixture composition at a specific controlled pressure and a temperature of 40°C. With first sample taken from the reactor, the reading of the humidity sensor would indicate accurately the water mass content of the mixture in the reactor. A sample taken from the reactor undergoing chromatographic analysis will indicate the precise mixture composition. The uncertainty in the mixtures composition measurements using the GC (Gas Chromatography) is 0.01%. The uncertainty in the temperature measurement inside the cell is 0.5 °C and that of the pressure is 0.3%.

With initial soluble water conditions, the sampling process starts. In every sample (flow rate 50ml/min for a couple of minutes), 0.1 to 0.2g of CO₂ are taken out from the reactor. The water content of the sample is measured using the humidity analyzer and compared to the first reading. Pressure

in the reactor is kept constant (dropping the piston level of 1-3% of the cell height when it is full of liquid), whereas the temperature is dropped after each sample using the heat exchanger. The sampling process continues dropping each time the temperature inside the reactor while maintaining the same initial pressure until the humidity analyzer reads lower reading. The drop in the water mass content in the sample is explained by the formation of free water on the reactor wall, indicating that water dew-point temperature is reached. The uncertainty in the detection of the dew-point is 1.2°C.

IV. MODELS

The models used for comparison with the experimental data are the GERG-2008 [10], and the EOS-CG [11] equations of state.

The GERG-2008 and EOS-CG models are based on the same multi-fluid approach but use different adjusted mixture parameters. They are explicit in the reduced Helmholtz free energy $\alpha = a(\rho, T, \bar{x})/RT$, which is a function of density ρ , temperature T , and mixture composition (or mole fraction) \bar{x} (R is the gas constant). It can be expressed by an ideal-gas part α^0 and a residual contribution α^r according to the following equation:

$$\alpha(\delta, \tau, \bar{x}) = \frac{a}{RT} = \alpha^0(\rho, T, \bar{x}) + \alpha^r(\delta, \tau, \bar{x}) \quad (1)$$

where the reduced mixture density δ and the inverse reduced mixture temperature τ are given by

$$\delta = \rho / \rho_r(\bar{x}) \text{ and } \tau = T_r(\bar{x}) / T \quad (2)$$

According to [10], the functional form of the reducing functions $\rho_r(\bar{x})$ and $T_r(\bar{x})$ is given by

$$\frac{1}{\rho_r(\bar{x})} = \sum_{i=1}^N x_i^2 \frac{1}{\rho_{c,i}} + \sum_{i=1}^{N-1} \sum_{j=i+1}^N 2x_i x_j \beta_{v,ij} \gamma_{v,ij} \frac{x_i + x_j}{\beta_{v,ij}^2 x_i + x_j} \frac{1}{8} \left(\frac{1}{\rho_{c,i}^{1/3}} + \frac{1}{\rho_{c,j}^{1/3}} \right)^3 \quad (3)$$

and

$$T_r(\bar{x}) = \sum_{i=1}^N x_i^2 T_{c,i} + \sum_{i=1}^{N-1} \sum_{j=i+1}^N 2x_i x_j \beta_{T,ij} \gamma_{T,ij} \frac{x_i + x_j}{\beta_{T,ij}^2 x_i + x_j} (T_{c,i} T_{c,j})^{0.5} \quad (4)$$

with adjustable binary reducing parameters $\beta_{v,ij}$, $\gamma_{v,ij}$, $\beta_{T,ij}$, and $\gamma_{T,ij}$ and the critical densities and temperatures ρ_c and T_c of the pure components in the mixture.

While the residual part α^r of the Helmholtz free energy model is evaluated at reduced mixture parameters, using composition-dependent reducing functions $\rho_r(\bar{x})$ and $T_r(\bar{x})$, the ideal-gas part α^0 is evaluated at the non-reduced density ρ and temperature T . It is given by

$$\alpha^0(\rho, T, \bar{x}) = \sum_{i=1}^N x_i \left[\alpha_{0,i}^0(\delta_{0,i}, \tau_{0,i}) + \ln x_i \right] \quad (5)$$

where N is the number of components in the mixture and $\alpha_{0,i}^0$ and x_i are the dimensionless ideal-gas part of the Helmholtz free energy and the mole fraction of component i in the mixture. The sum $x_i \ln x_i$ accounts for the entropy of mixing in the ideal mixture. The ideal-gas parts of the Helmholtz free energies of each pure component are evaluated at their component specific reduced parameters $\delta_{0,i}$ and $\tau_{0,i}$, which are given by

$$\delta_{0,i} = \rho / \rho_{c,i} \text{ and } \tau_{0,i} = T_{c,i} / T. \quad (6)$$

The residual part of the Helmholtz free energy of the mixture is given by

$$\alpha^r(\delta, \tau, \bar{x}) = \sum_{i=1}^N x_i \alpha_{0,i}^r(\delta, \tau) + \Delta \alpha^r(\delta, \tau, \bar{x}) \quad (IV7)$$

where $\alpha_{0,i}^r$ is the residual part of the reduced Helmholtz free energy of component i and $\Delta \alpha^r$ is the so-called *departure function*, which is constituted by

$$\Delta \alpha^r(\delta, \tau, \bar{x}) = \sum_{i=1}^{N-1} \sum_{j=i+1}^N x_i x_j F_{ij} \alpha_{ij}^r(\delta, \tau) \quad (8)$$

with the binary departure function α_{ij}^r for the components i and j and the weighing factor F_{ij} introduced by [10]. The mathematical structure of the binary departure function used in the GERG-2008 model is a combination of polynomial and exponential terms especially developed for mixtures. It reads

$$\alpha_{ij,GERG-2008}^r(\delta, \tau) = \sum_{k=1}^{K_{pol,ij}} n_{ij,k} \delta^{d_{ij,k}} \tau^{t_{ij,k}} + \sum_{k=K_{pol,ij}+1}^{K_{pol,ij}+K_{exp,ij}} n_{ij,k} \delta^{d_{ij,k}} \tau^{t_{ij,k}} \exp \left[-\eta_{ij,k} (\delta - \varepsilon_{ij,k})^2 - \beta_{ij,k} (\delta - \gamma_{ij,k}) \right] \quad (9)$$

Additionally to this structure, the departure function in the EOS-CG model uses a simple form of exponential terms also used in common Helmholtz models for pure fluids. It is given by

$$\alpha_{ij,EOS-CG}^r(\delta, \tau) = \sum_{k=1}^{K_{pol,ij}} n_{ij,k} \delta^{d_{ij,k}} \tau^{t_{ij,k}} + \sum_{k=K_{pol,ij}+1}^{K_{pol,ij}+K_{exp,ij}} n_{ij,k} \delta^{d_{ij,k}} \tau^{t_{ij,k}} \exp(-\delta^{d_{ij,k}}) + \sum_{k=K_{pol,ij}+K_{exp,ij}+1}^{K_{pol,ij}+K_{exp,ij}+K_{exp,ij}} n_{ij,k} \delta^{d_{ij,k}} \tau^{t_{ij,k}} \exp \left[-\eta_{ij,k} (\delta - \varepsilon_{ij,k})^2 - \beta_{ij,k} (\delta - \gamma_{ij,k}) \right] \quad (10)$$

The mixture models given in (1) to (10) are thus a combination of pure fluid contributions, namely $\alpha_{0,i}^0$ and $\alpha_{0,i}^r$, and mixture contributions, namely the reducing functions $\rho_r(\bar{x})$ and $T_r(\bar{x})$, and the binary departure functions α_{ij}^r . For the description of the pure fluid contributions [10] developed new short Helmholtz equations of state specifically designed

to work well with mixture models, while in the EOS-CG model the established reference Helmholtz equations were used. The models are adjusted to experimental mixture data by fitting the binary reducing parameters $\beta_{v,ij}$, $\gamma_{v,ij}$, $\beta_{T,ij}$, $\gamma_{T,ij}$ and, if necessary, the adjustable parameters in the binary departure function α_y^r .

The experimental data used for the parameter fitting of the EOS-CG model include properties in the homogeneous gas and liquid phase (densities, speed of sound data, heat capacities or excess enthalpies) as well as phase equilibrium measurements (phase compositions at given temperature and pressure) over a wide temperature, pressure and composition range. The parameters were fitted by minimizing the sum of squares of the deviations between experimental and calculated property values, using a non-linear optimization algorithm. This method enables fitting to all kinds of available experimental data simultaneously without any pre-correlations [11].

V. EXPERIMENTAL AND SIMULATION RESULTS

A. Experimental Data

The water solubility experimental data obtained for pure CO₂ and for CO₂-N₂ mixtures are given in Figs. 3 (a) and (b) respectively. The figure shows that water solubility is dependent on temperature and pressure. The solubility tends to increase for all mixtures tested with the increase of the temperature. For example, with pure CO₂ and at constant pressure conditions of 120 bar, the experimental data show an increase in the water solubility from close to 1025 ppm at 15°C, to around 1470 ppm at 28°C and up to 2100 ppm at 38°C. At similar pressure conditions of 120 bar, the solubility of water in the CO₂-N₂ mixtures increased from 975 ppm at 16°C, to around 1480 ppm at 30°C and up to around 1990 ppm at 39°C.

The solubility is also influence by the mixture pressure. With similar temperature conditions, higher mixture pressure results in higher maximum water solubility limits. This behaviour was also observed for all mixtures tested. For example, at 17°C, pure CO₂ can absorb up to 990 ppm (in the soluble state) at 90 bar, 1100 ppm with 120 bar conditions and close to 1250 ppm at 150 bar. A similar trend is observed with the CO₂-N₂ mixtures. At 20°C, a mixture of CO₂ with 2.5% N₂ can absorb up to 1000 ppm at 90 bar, around 1120 ppm at 120 bar and close to 1240 ppm at 150 bar. The increase in the solubility driven by the increase in the pressure has been observed for all measured mixtures temperatures.

The experimental investigation with the mixtures containing 500 ppm of water showed that the 500 ppm of water was still fully soluble at the lowest pressure (90 bar) and temperature (5°C) conditions that could be achieved in the test set up, for the different tested mixtures.

Fig. 4 compares the water solubility measured in pure CO₂ to that measured in mixtures of CO₂ with nitrogen or with oxygen. A similar dependency on temperature and pressure is observed with the different mixtures. However, the results show a drop in the water solubility limit with the presence of

those impurities. Similar or close water solubility data were observed with both mixtures (CO₂-N₂ and CO₂-O₂ mixtures). At the different pressures and temperatures tested, the presence of 2.5% N₂ or 2.5% O₂ in CO₂ lowers the water solubility limit from 75 ppm up to 150 ppm depending on pressure and temperature.

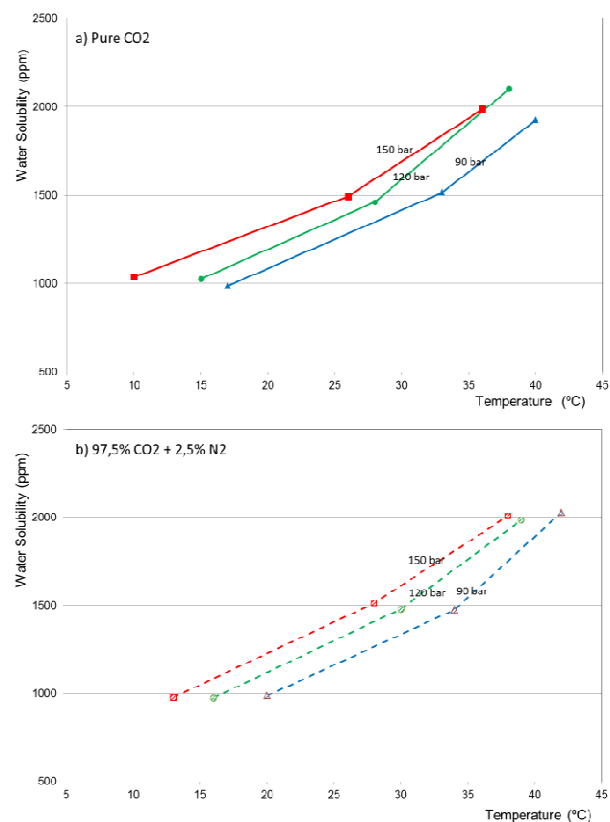


Fig. 3 Water solubility in pure CO₂ (a) and in CO₂-N₂ (b) mixture as function of temperature for different three fixed pressures (isobars)

This drop in water solubility due to the presence of impurities will have serious implication on the CO₂ pipeline design and on the CO₂ mixtures specifications at the capture locations especially that higher percentage of impurities might be expected in the CO₂ captured stream. Thus, with the presence of impurities either higher minimum pressures or higher minimum temperatures should be maintained in the pipeline or less water should be allowed to avoid free water formations and corrosion problems.

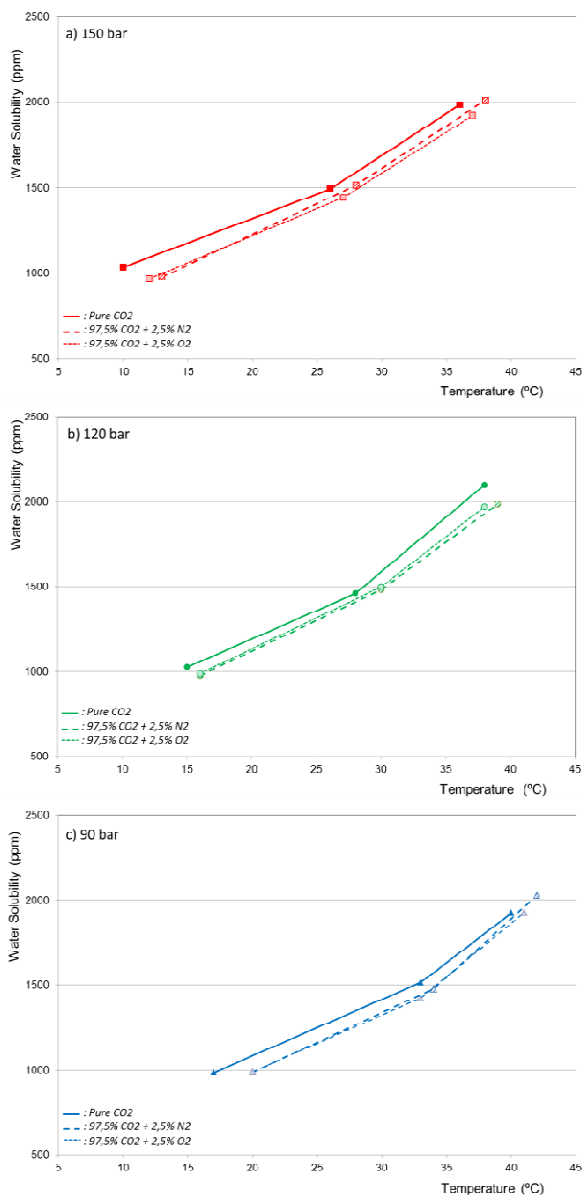


Fig. 4 Influence of impurities on water solubility

B. Model Calculations

In Fig. 5 the experimental data obtained for water solubility in pure CO₂ (Fig. 5 (a)) and in CO₂-N₂ (Fig. 5 (b)) mixture are compared to the predictions of the two models, the GERG-2008 and the EOS-CG. The GERG-2008 equation of state shows better predictions of water solubility.

The GERG-2008 model predicts well the dependency of water solubility as function of pressure and temperature. Figs. 5 (a) and (b) show that at relatively low temperatures (28°C and lower) and higher pressures (120 and 150 bar) good agreement is observed between the calculations and measurements; comparison with experimental data shows an average prediction error of less than 100 ppm for the different measurement points. At higher temperatures (28°C and above) and at lower pressures (90 bar) approaching the critical zone, the model performance deteriorates. This could be seen in the

over-estimation of water solubility in pure CO₂ of more than 250 ppm at 90 bar and 33°C in the under-estimation of water solubility in CO₂-N₂ mixtures of more than 500 ppm at 90 bar and 42°C.

The EOS-CG model shows the right trend predicting the water solubility in both mixtures as function of pressure and temperature except at low pressure of 90 bar (closest to the critical pressure) where an increase in temperature results in a drop of water solubility. However and in comparison with the GERG-2008 model, the EOS-CG model substantially overestimates the solubility of water in both pure CO₂ and in CO₂ mixtures and for the different pressures and temperature examined. The EOS-CG model calculations (Fig. 5) show a prediction error that reaches 400% with a remarkably better performance at 90 bar and at high temperatures.

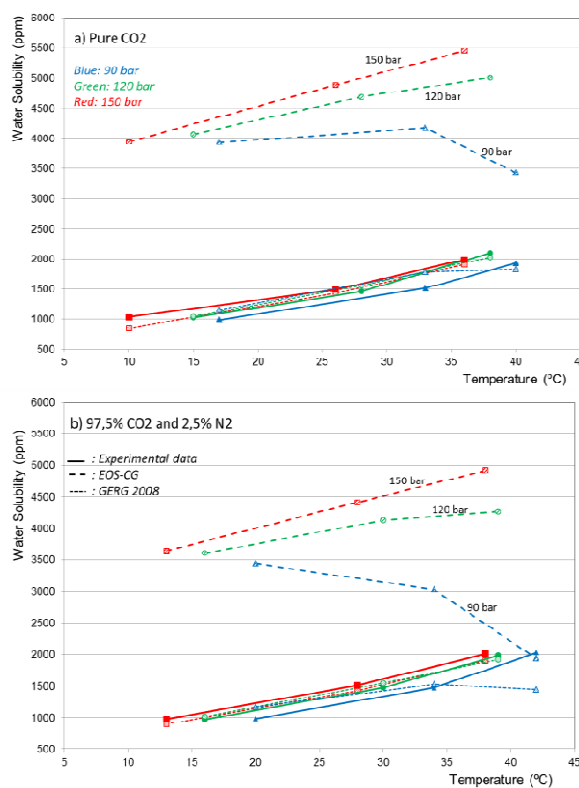


Fig. 5 Water solubility in pure CO₂ and in CO₂-N₂ mixtures - Models prediction and experimental data. Solid Line: experimental data, dashed line: EOS-CG, square dot: GERG 2008. (Blue: 90 bar, Green: 120 bar, Red: 150 bar)

VI. CONCLUSION

The solubility of water in CO₂ has been studied. The influence of having impurities on water solubility has been experimentally examined. The capabilities of two mixture models, the GERG-2008 model and the EOS-CG model, were assessed using the experimental data. The generated data and the different models predictions have been analyzed and the following conclusions can be made:

- The water solubility is dependent on temperature and pressure. The solubility tends to increase for all mixtures tested with increasing temperatures and/or pressures.
- Measurements showed that all tested mixtures with water fractions 500 ppm were fully soluble at the lowest measured pressure (90 bar) and temperature (5 °C)
- The measurements showed a drop in the water solubility limit from 75 ppm up to 150 ppm with the presence of 2.5% of N₂ or 2.5% of O₂.
- The GERG-2008 equation of state showed better predictions of water solubility in comparison with the EOS-CG model; however, deterioration in the performance is observed close to the critical zone.

ACKNOWLEDGMENT

This project is funded by the Energy Delta Gas Research programme (EDGaR).

REFERENCES

- [1] H. Van Dijk. Edgar CO₂ purity: types and quantities of impurities related to CO₂ point source and capture technology. ECN report: ECN-E-12-054, 2012.
- [2] A. Chapoy, R. Burgass, B. Tohidi, J.M. Austell and C. Eickhoff C. Effect of Common Impurities on the Phase Behavior of Carbon-Dioxide-Rich Systems: Minimizing the Risk of Hydrate Formation and Two-Phase Flow. SPE Journal. Volume 16, Number 4, 2011.
- [3] E. Goos, U. Riedel, L. Zhao and L. Blum. Phase diagrams of CO₂ and CO₂- N₂ gas mixtures and their application in compression processes. Energy Procedia 4, 3778-3785, 10th International Conference on Greenhouse Gas Control Technologies, 2011.
- [4] M. Seiersten, Material selection for separation, transportation and disposal of CO₂, Proceedings Corrosion, National Association of Corrosion Engineers, paper 01042, 2001.
- [5] E. De Visser, C. Hendriks, M. Barrio, M. Molnvik, G. de Koeijer, S. Liljemarkand Y. Le Gallo. DynamisCO₂ quality recommendations”, International Journal of Greenhouse Gas Control 2, 478 – 484, 2008.
- [6] M. Mohitpour, H. Golshan and A. Murray. *Pipeline Design & Construction*, A practical approach, The American Society of Mechanical Engineers, Three Park Avenue, New York, United States, 2003.
- [7] P. Odru, P. Broutin, A. Fradet, S. Saysset, J. Ruerand L. Girod. Technical and economic assessment of CO₂ transportation, Institute France Petrole, GHGT-8, Trondheim, 2006.
- [8] A. Austegard and M. Barrio. Project Internal Memo DYNAMIS: Inert components, solubility of water in CO₂ and mixtures of CO₂ and CO₂ hydrates, 2006.
- [9] A. Austegard, E. Solbraa, G. de Koeijer G and M.J. Mølrvik. Thermodynamic Models for Calculating Mutual Solubilities in H₂O-CO₂-CH₄ mixtures. Chemical Engineering Research and Design (ChERD), Part A, 2005. Special issue: Carbon Capture and Storage, V 84, A9, pp. 781-794, 2006.
- [10] O. Kunz, and W. Wagner. The GERG-2008 Wide-Range Equation of State for Natural Gases and Other Mixtures: An Expansion of GERG-2004. Journal Chem. Eng. Data 57, 3032–3091, 2012.
- [11] J. Gernert. A New Helmholtz Energy Model for Humid Gases and CCS mixtures, Dissertation, Ruhr-Universität Bochum, 2013.